



## *Supplement of*

# **Aerosols over continental Portugal (1978–1993): their sources and an impact on the regional climate**

**A. L. Morozova and I. A. Mironova**

*Correspondence to:* A. L. Morozova ([annamorozovauc@gmail.com](mailto:annamorozovauc@gmail.com), [anna\\_m@teor.fis.uc.pt](mailto:anna_m@teor.fis.uc.pt))

The copyright of individual parts of the supplement might differ from the CC-BY 3.0 licence.

## Part 1. Data

### 1.1 Aerosol parameters

The Nimbus-7 satellite with the TOMS instrument onboard was launched on October 1978 and operated continuously for 14.5 years until TOMS failed in May 1993. The TOMS AI series have gaps: 80 days are missed for the site ID 082 (1.5% of the whole data set length) and 88 days are missed for the site ID 288 (1.7% of the whole data set length). The TOMS instrument measures the integrated over the atmospheric column amount of the UV light scattered by airborne particles. Data from TOMS can be used to detect the presence of both UV absorbing and non-absorbing (mostly scattering) aerosols in the atmosphere. The UV absorbing aerosols include particles produced by e.g. Saharan dust, forest fires or volcanic eruptions. Non-absorbing aerosols are primarily tiny sulfate and nitrate aerosols produced, mostly, by human activities. Aerosol index is positive when UV absorbing aerosols prevail and AI negative in case of prevailing of non-UV absorbing aerosols. Quantitatively, the TOMS aerosol index AI is defined as (Hsu et al., 1999)

$$AI = -100(\log_{10}[I_{\lambda}/I_{\lambda_0}]_{meas} - \log_{10}[I_{\lambda}/I_{\lambda_0}]_{calc}), \quad (S1)$$

where  $I_{meas}$  is the backscattered radiance at wavelengths measured by the TOMS instrument and  $I_{calc}$  is the model calculated radiance assuming an atmosphere of Rayleigh scatterers (pure molecular atmosphere) for two close wavelength  $\lambda$  and  $\lambda_0$  in UV region (Ginoux and Torres, 2003). When UV absorbing aerosols are present in the atmosphere, the spectral contrast  $I_{\lambda}/I_{\lambda_0}$  is smaller than predicted by the calculation model, and the equation (S1) produces positive residues. Non-absorbing aerosols produce greater spectral contrast, and thus result in a negative value of AI.

#### Spatial correlation between the AI sites.

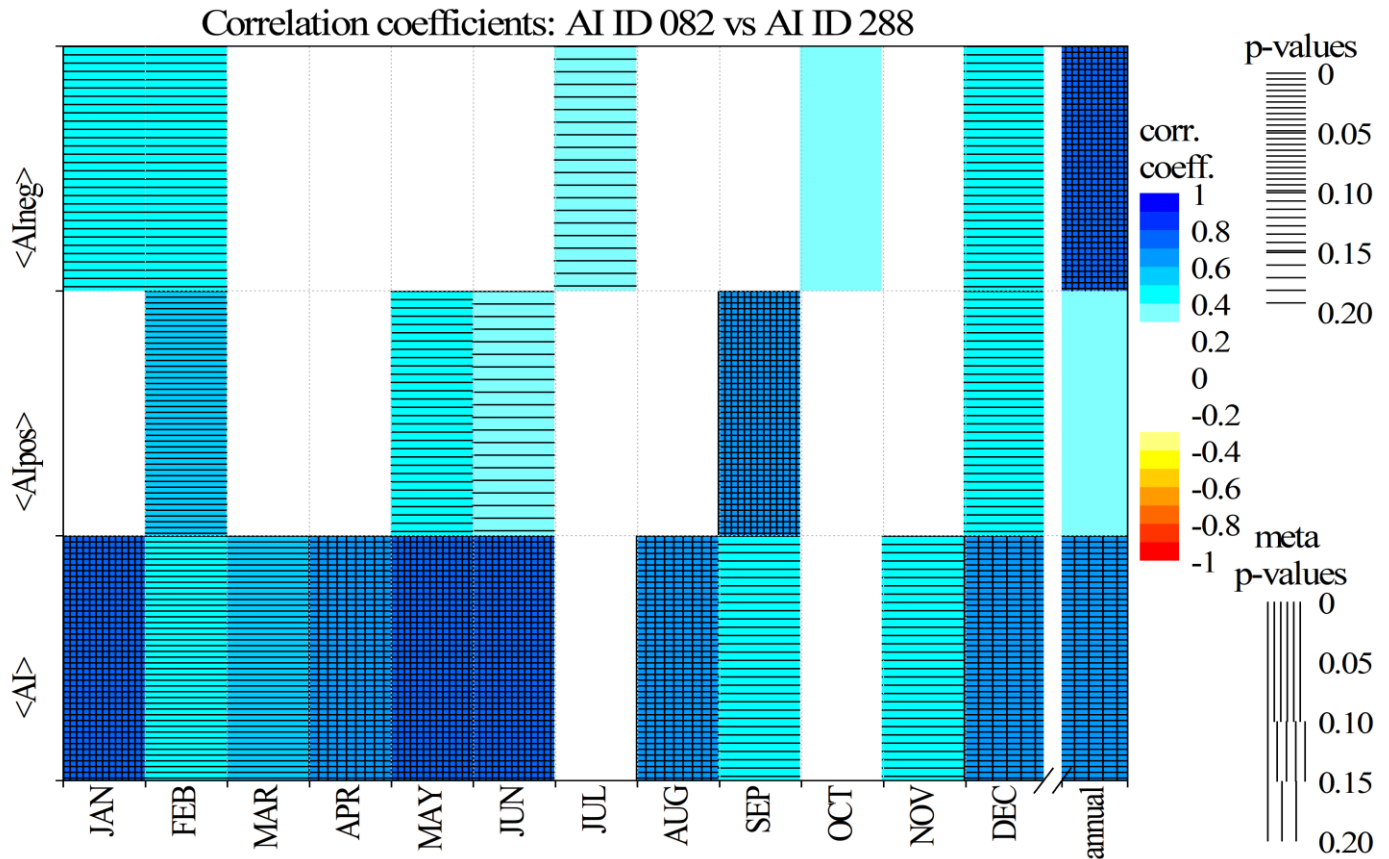


**Figure S1.1.** Correlation coefficients ( $r$ ) between the AI indices measured at two aerosol sites ID 082 and ID 288. Only correlation coefficients  $|r| \geq 0.3$  are shown. The statistical significances for singular ( $p$  values) and multiple (meta  $p$  values) comparisons are shown by shading. The highest correlations are between the <AI> series. The correlations coefficients for the <Alpos> series are higher for the monthly series, and for the <Alneg> series are higher for the annual series.

## 1.2 Atmospheric parameters

The IGUC and IGIDL series of different parameters have different length, but all of them are available for the studied period. The temperature and pressure series already have passed through the homogenization procedure and are considered free from the significant artificial homogeneity breaks (see Morozova and Valente (2012), Bližňák et al. (2014), Stickler et al. (2014) for details). The other digitalized series were checked for OCR errors and misprints. Afterward, the homogeneity of these series was analysed using standard homogeneity tests (same as used in Morozova and Valente, 2012), and a number of probably artificial homogeneity breaks were found. Fortunately, none of these breaks took place during the relatively short studied period. Therefore, these series were used without any correction.

Since the distance between the aerosol detection site and the meteorological station in the pair “IGUC series plus AI series for the rural site ID 288” is about 74 km and therefore is quite large, we compared the data from IGUC with the data from the meteorological station at Pehnas Douradas (located very close to the AI site ID 288) available at Global Historical Climatology Network data base (<http://www.ncdc.noaa.gov/ghcnm/>, station ID 8568). This dataset contains data on monthly means of daily mean temperature, pressure re-calculated to the sea-level and precipitation amount. These series are quite short, fragmented and do not fully cover the AI measurement period. However, they are highly correlated with the corresponding IGUC series as is seen in Fig. S1.2. Therefore, we decided to use only IGUC series that have no gaps, for which we can obtain all metadata information and perform all necessary homogeneity tests.

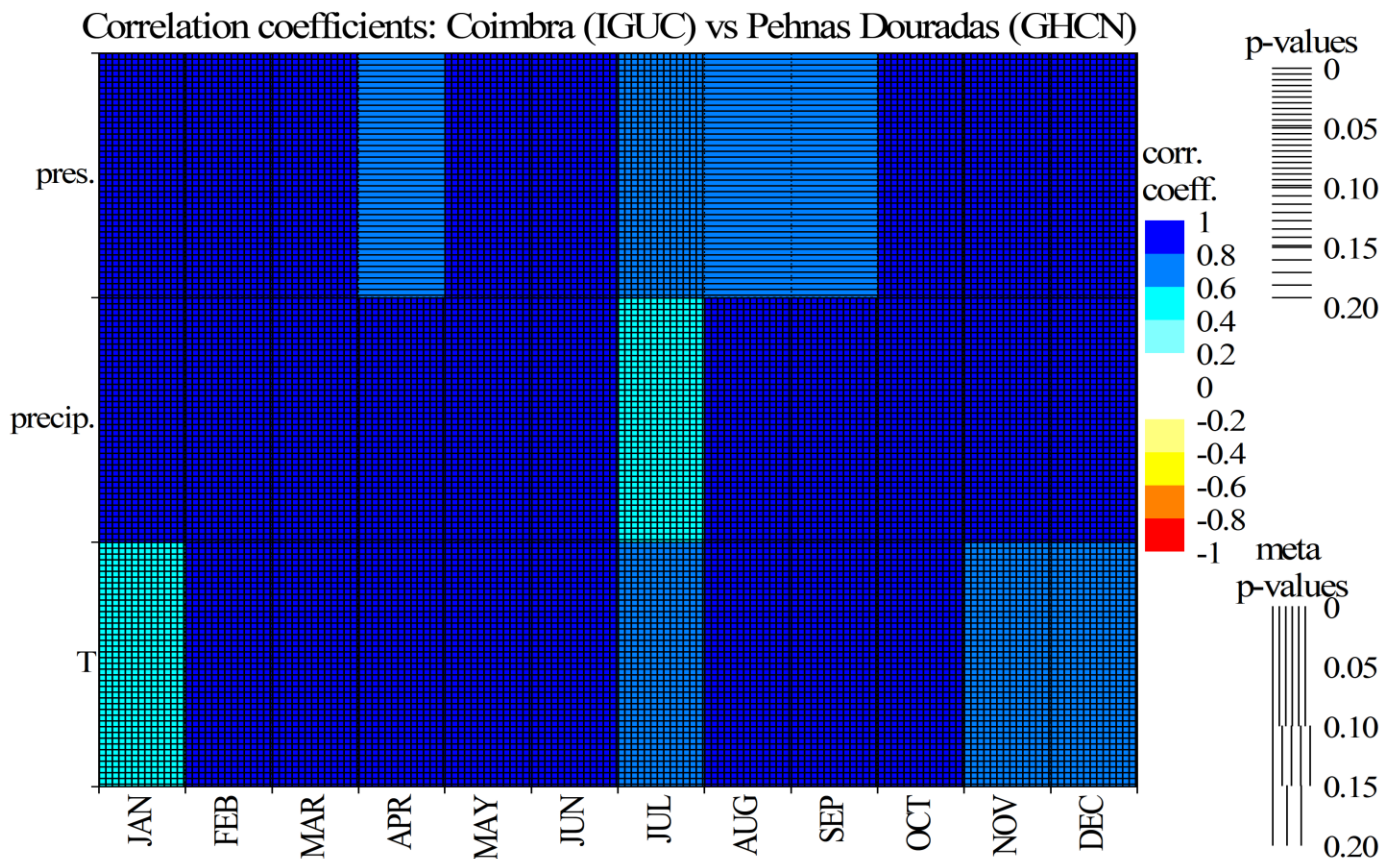


**Figure S1.2.** Correlation coefficients ( $r$ ) between the atmospheric parameters measured in Coimbra (IGUC series) and Pehnas Douradas (Global Historical Climatology Network series). Only correlation coefficients  $|r| \geq 0.3$  are shown. The statistical significances for singular ( $p$  values) and multiple (meta  $p$  values) comparisons are shown by shading.

## Correlation between the IGUC and IGIDL climatic series

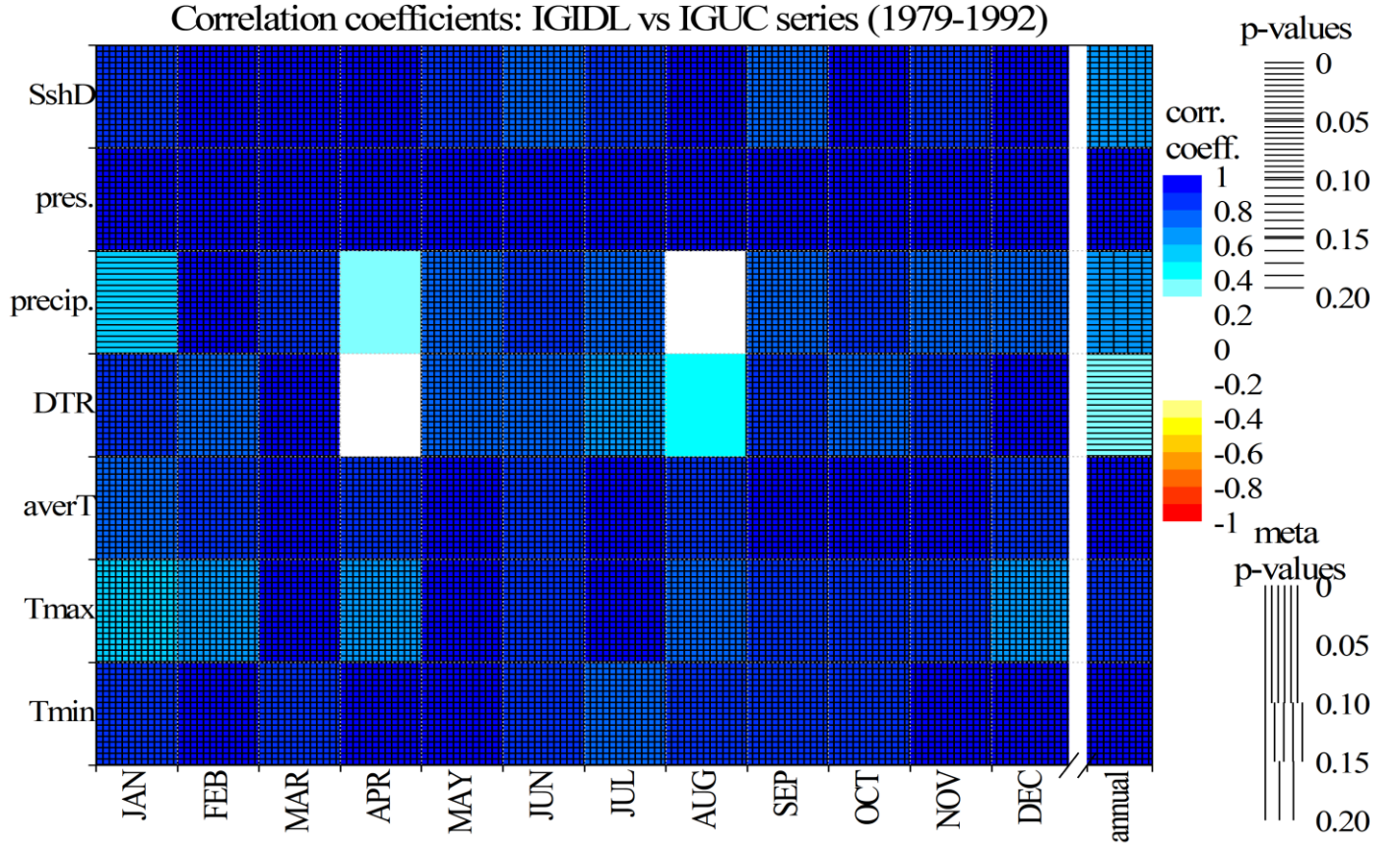


**Figure S1.3.** Correlation coefficients ( $r$ ) between the atmospheric parameters measured in Coimbra (IGUC series) and Lisbon (IGIDL series). Only correlation coefficients  $|r| \geq 0.3$  are shown. The statistical significances for singular ( $p$  values) and multiple (meta  $p$  values) comparisons are shown by shading.

### 1.3 Aerosol sources

**Saharan Dust Events (SDE).** In this work we identified SDE as described in Barkan et al. (2005) and Varga et al. (2013). The Saharan dust event is defined as a day when a standardized AI ( $AI_{st}$ , see Eq. S2) is not less than 3.5. The daily AI series were standardized separately for each year to reduce their annual means ( $AI_{mean}$ ) to 0 and standard deviations ( $\sigma_{AI}$ ) to 1 (see Barkan et al., 2005).

$$AI_{st} = (AI - AI_{mean}) / \sigma_{AI}, \quad (S2)$$

Considering that we did not use satellite images for the SDE identification, we cannot guarantee that all the events detected by above mentioned method are the real SDEs. We also could have missed some events. To test our SDE list, we compared monthly/annual sums of our SDEs for both Portuguese sites with similar published data for regions more or less close to Portugal:

1. number of the Saharan dust events in July from Brakan et al. (2005) – Italy;
2. annual sums of the SDE from Rogora et al. (2004) – NW Italy;
3. annual sums of the SDE from Varga et al. (2013) – Carpathian Basin.

The results of the comparison are shown in Fig. S1.4b-d. The number of dust events detected by us for the site ID 288 correlate well with other data. Correlation coefficients are 0.48 and 0.56 for annual data and 0.89 for monthly ( $p$  values for all correlation coefficients a lower than 0.01). The number of the SDEs for the site ID 082 shows a very weak (if any) correlation with other series. Figure S1.4a shows as well the annual cycle for the monthly sums of the SDEs detected in our study for both locations. As expected, July and August are months of the highest frequency of SDEs.



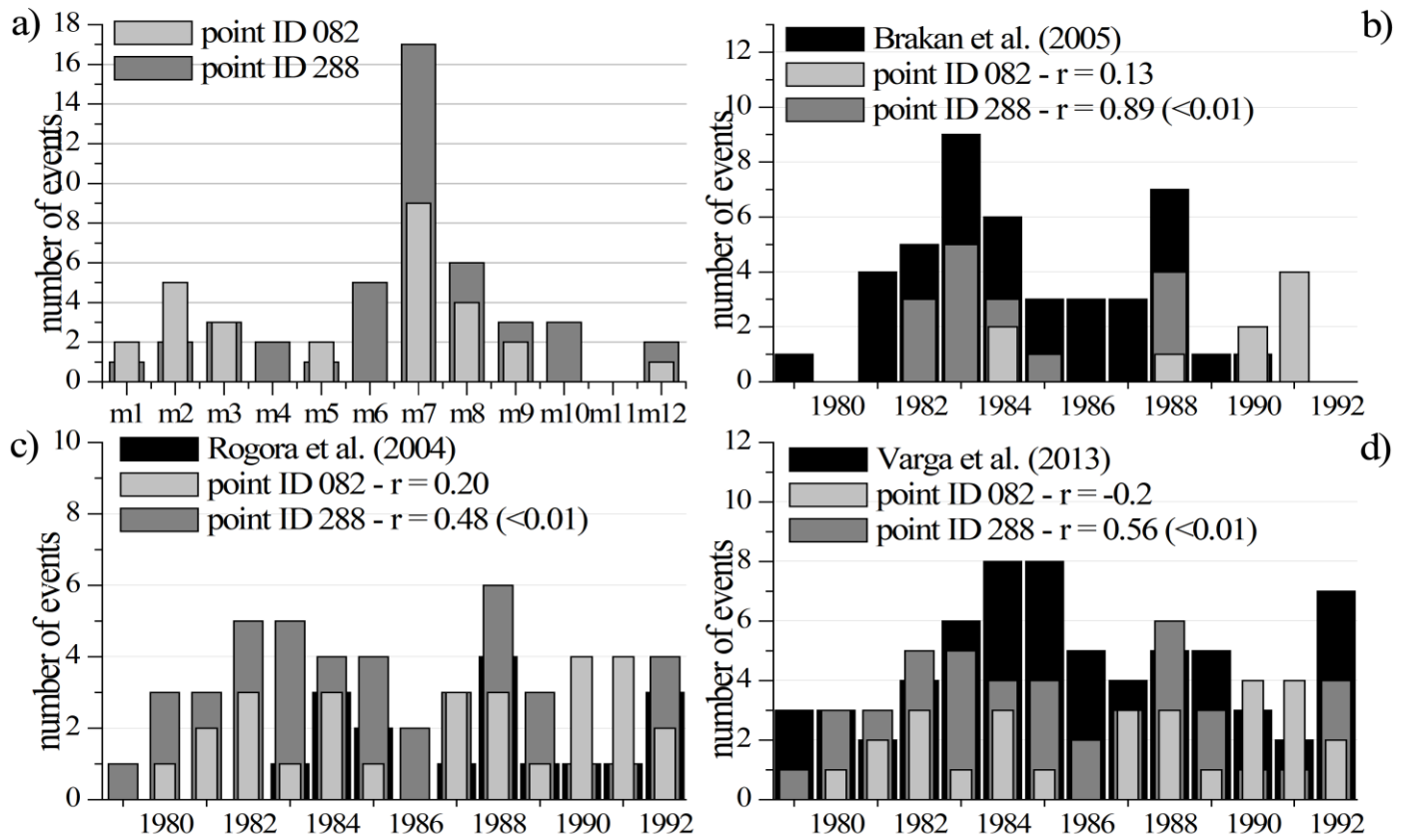


**Figure S1.4.** (a) Annual cycle of the monthly number of SDE for Portuguese sites ID 082 and ID 288. (b-d) Variations of the monthly (b) and annual (c-d) SDE number for two Portuguese sites compared to the equivalent data from other studies. The correlation coefficients  $r$  between the monthly/annual sums of the SDE events detected by us and by other authors are shown with  $p$  values in brackets.

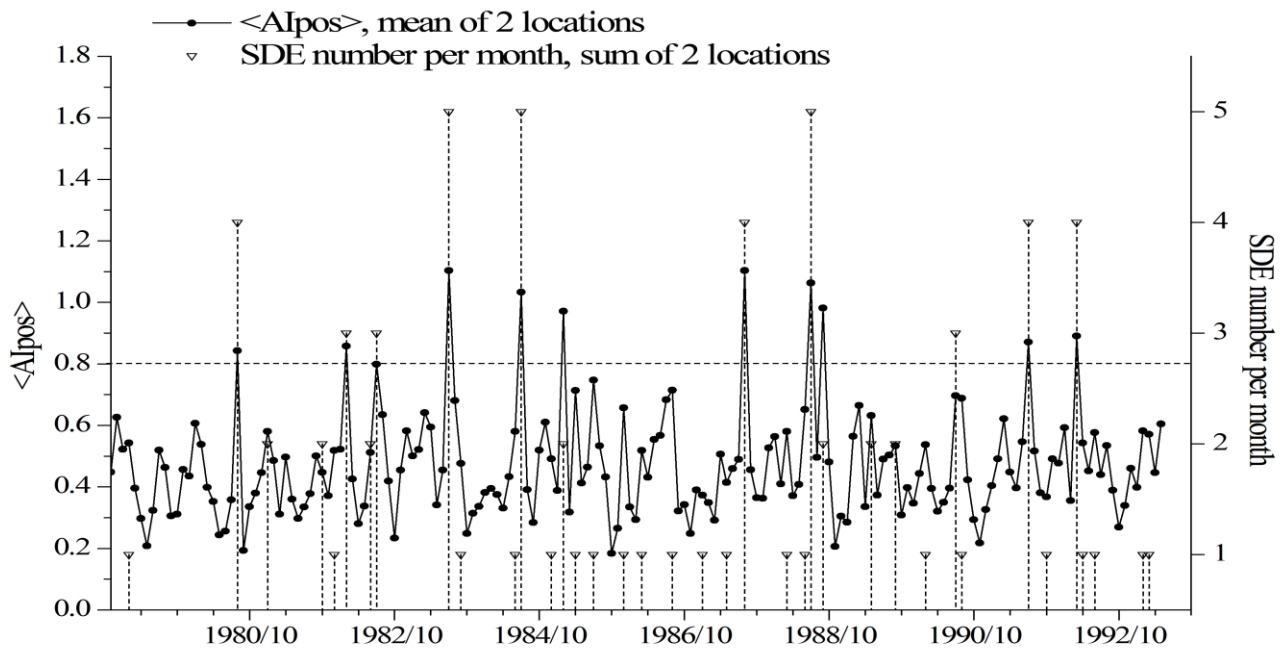


**Figure S1.5.** Series of monthly  $\langle \text{Alpos} \rangle$  (a mean for two sites ID 082 and ID 288) and a total number of SDE per month for the same sites.

The sites ID 082 and ID 288 were analysed separately. During the studied period 28 SDEs were found for the site ID 082 and 45 SDEs were found for the site ID 288 (see Fig. 2d of the main paper). As was previously shown by different studies (see e.g. Moulin et al., 1998, Barkan and Alpert, 2008 or Israelevich et

al., 2012), most frequent routs for the dust intrusions coming from Sahara to the west part of the Iberian Peninsula pass through the west part of the Mediterranean sea and Spain or along a west-east line after overpassing the North Atlantic Ocean (e.g. Pereira et al. 2008, 2011). Thus, a greater number of SDEs for the site ID 288 is due to its more north-east position. This hypothesis is confirmed by the fact that in cases when the SDE is observed on both sites more or less simultaneously, on the site ID 288 it took place 1-3 days earlier than on the site ID 082.

High daily values of the  $\langle \text{AIpos} \rangle$  during the detected SDEs contribute to the increase of monthly means of the  $\langle \text{AIpos} \rangle$ . The variations of the monthly mean  $\langle \text{AIpos} \rangle$  index averaged over two Portuguese locations increase together with the total monthly number of dust events are shown in Fig. S1.5. Months with a very high content of absorbing aerosols ( $\langle \text{AIpos} \rangle \geq 0.8$  for averaged data) are months with at least three SDEs. There are two exceptions (February 1985 and September 1988). During these months only two SDEs took places, but the monthly  $\langle \text{AIpos} \rangle$  is over 0.8. In both cases one of the pair of SDEs was an extremely strong event. No relations were found between the  $\langle \text{AI}_{\text{neg}} \rangle$  and the SDE occurrences.

## References

- Barkan, J., Alpert, P., Synoptic patterns associated with dusty and non-dusty seasons in the Sahara. *Theoretical and Applied Climatology*, 94, 3-4, 153-162, 2008.
- Barkan, J.; Alpert, P.; Kutiel, H.; Kishcha, P.: Synoptics of dust transportation days from Africa toward Italy and central Europe. *JGR: Atmospheres*, Volume 110, Issue D7, CiteID D07208, 2005.
- Bližňák, V., Valente, M. A., & Bethke, J. Homogenization of time series from Portugal and its former colonies for the period from the late 19th to the early 21st century. *Int. J. Climatol*, doi: 10.1002/joc.4151, 2014.
- Ginoux, P., Torres, O.: Empirical TOMS index for dust aerosol: Applications to model validation and source characterization, *JGR: Atmospheres* (1984–2012), 108(D17), 4534, doi:10.1029/2003JD003470, 2003.
- Hsu, N. C., Herman, J. R., Torres, O., Holben, B. N., Tanre, D., Eck, T. F., Smirnov, A., Chatenet, B., and Lavenu, F.: Comparisons of the TOMS aerosol index with Sunphotometer aerosol optical thickness: Results and applications, *J. Geophys. Res.*, 104, 6269–6279, doi: 10.1029/1998JD200086, 1999.
- Israelevich, P., Ganor, E., Alpert, P., Kishcha, P., Stupp, A.: Predominant transport paths of Saharan dust over the Mediterranean Sea to Europe. *J. Geophys. Res.: Atmos.*, 117, D2, CiteID D02205, 2012.
- Morozova, A. L. and Valente, M. A.: Homogenization of Portuguese long-term temperature data series: Lisbon, Coimbra and Porto, *Earth Syst. Sci. Data*, 4, 187-213, 2012.
- Moulin, C., Lambert, C. E., Dayan, U., Masson, V., Ramonet, M., Bousquet, P., Legrand, M., Balkanski, Y. J., Guelle, W., Marticorena, B., Bergametti, G., Dulac, F., Satellite climatology of African dust transport in the Mediterranean atmosphere. *JGR: Atmospheres*, 103, D11, 13,137-13,144, 1998.
- Pereira, S., Wagner, F., Silva, A.M.: Scattering properties and mass concentration of local and long-range transported aerosols over the South Western Iberia Peninsula, *Atmos. Environ.*, 42, 33, 7623-7631, 2008.
- Pereira, S.N., Wagner, F., Silva, A.M.: Seven years of measurements of aerosol scattering properties, near the surface, in the southwestern Iberia Peninsula, *Atmospheric Chemistry and Physics*, 11, 1, 17-29, 2011.
- Rogora, M., Mosello, R., Marchetto, A., Long-term trends in the chemistry of atmospheric deposition in Northwestern Italy: the role of increasing Saharan dust deposition, *Tellus B*, 56, 5, 426-434, 2004.
- Stickler, A., Brönnimann, S., Valente, M. A., Bethke, J., Sterin, A., Jourdain, S., Roucaute, E., Vasquez, M.V., Reyes, D.A., R. Allan, R., Dee, D. ERA-CLIM: historical surface and upper-air data for future reanalyses. *Bull. Amer. Meteorol. Soc.*, 95(9), 1419-1430, doi: <http://dx.doi.org/10.1175/BAMS-D-13-00147.1>, 2014.
- Varga, G., Kovács, J., Újvári, G.: Analysis of Saharan dust intrusions into the Carpathian Basin (Central Europe) over the period of 1979-2011. *Global and Planetary Change*, 100, 333-342, 2013.

## Part 2. Sunshine duration variations

Figure S2.1 shows the correlation coefficients between the variations of the sunshine duration (*SshD*) and other atmospheric parameters. As one can see, the *SshD* series is strongly anti-correlates with precipitations amount (a proxy for the cloud amount) and correlate with the atmospheric pressure (except summer dry months). In turn, the *DTR* series is affected by the *SshD* variations: the decrease of the sunshine duration coincides with the decrease of the daily temperature range. This results, most probably, from the decrease of the day-time temperature (*Tmax*) due to the lower amount of solar radiation. The correlation between the *SshD* and the atmospheric pressure is strong and statistically significant only during cold and wet season from October to March which is a sign of the Atlantic cyclones' effect (Miranda et al., 2002).

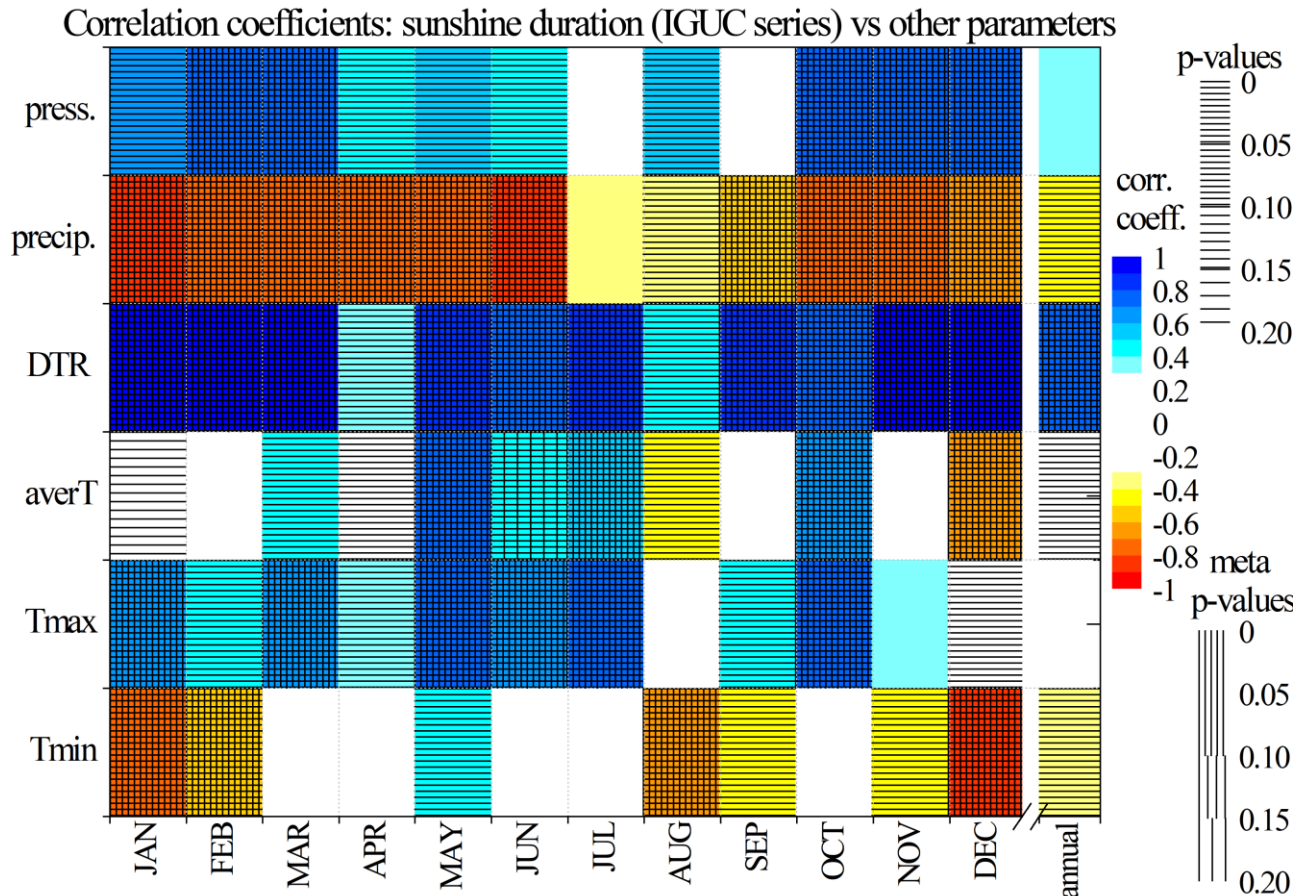


**Figure S2.1.** Correlation coefficients ( $r$ ) between the *SshD* and other atmospheric parameters measured in Coimbra (IGUC series). Only correlation coefficients  $|r| \geq 0.3$  are shown. The statistical significances for singular ( $p$ -values) and multiple (meta  $p$ -values) comparisons are shown by shading.

## References

Miranda, P., Coelho, F. E. S., Tomé, A. R., Valente, M. A., Carvalho, A., Pires, C., Pires, H. O., Pires, V. C., Ramalho, C.: 20th century Portuguese climate and climate scenarios, in: Climate Change in Portugal. Scenarios, Impacts and Adaptation Measures—SIAM Project, Santos FD, Forbes K, Moita R (Eds), Gradiva Publishers, Lisbon, 23-83, 2002.